



# Evaluation of Applicability of Some Algorithms for Controlling the Motion of Satellites in a Formation

Zaure Rakisheva,<sup>1</sup> Anna Sukhenko,<sup>1,2</sup> Nursultan Doszhan,<sup>1</sup> Gulama Garip Alisher Ibrayev,<sup>1</sup> Nazgul Kaliyeva,<sup>1,\*</sup> Shinichi Nakasuka<sup>3</sup> and Yerkin Shabdan<sup>4,\*</sup>

## Abstract

The remote sensing of Earth from a geostationary orbit can be achieved by deploying four independent spacecraft organized in a tetrahedral configuration. This innovative arrangement enables the substitution of a large optical telescope system. This paper delves into the challenges associated with studying the motion and maintenance of a tetrahedral formation of satellites in a geostationary orbit for Earth observation. To maintain the tetrahedral or regular pyramid configuration in an undisturbed reference orbit, algorithms based on the root locus method and feedback methods were developed. Through the course of this research, it was determined that these control methods for managing satellite motion within a formation could also be effectively applied to regulate the relative positions of satellites in a Fizeau interferometer configuration within geostationary orbits, particularly when utilizing modern electric propulsion systems.

**Keywords:** Spacecraft formation; Geostationary orbit; Tetrahedron configuration; Earth observation; Spacecraft formation control.

Received: 13 October 2023; Revised: 10 November 2023; Accepted: 14 November 2023.

Article type: Research article.

## 1. Introduction

The imperative to monitor emergencies such as fires and floods in real-time, given the vast expanse of our country, underscores the necessity of employing remote sensing spacecraft in high orbits. This paper suggests utilizing a formation of small spacecraft in geostationary orbit as a Fizeau interferometer to effectively cover the maximum possible area. Calculations demonstrate that, in specific scenarios, this configuration yields resolutions comparable to those achieved by spacecraft equipped with more costly optical systems.<sup>[1,2]</sup> The utilization of an interferometer enables the acquisition of high-quality images of the Earth's surface, using three or more satellites.<sup>[3-9]</sup>

We are considering a spacecraft formation utilizing an interferometer architecture, which consists of a system of four spacecraft arranged in a tetrahedron or regular pyramid.

As previously mentioned, this configuration offers improved coverage of the Earth's surface. It is worth noting that the study of tetrahedral formations in geostationary orbits has not received sufficient attention from researchers. This article specifically addresses studying the motion and maintaining of a tetrahedral formation of satellites in a geostationary orbit, emphasizing its application in constructing an interferometer. The assumption is made that the satellites are of a small scale (50 kg) to optimize project costs.

When considering the motion of satellites within a formation, selecting the correct form of dynamic equations and a coordinate system is crucial for the development of a control system that maintains the configuration of the formation. Numerous relative dynamic models have been derived using various approaches. The majority of spacecraft relative motion dynamic models are presented as direct ordinary differential equation models,<sup>[10-14]</sup> formulated in the Local-Vertical-Local-Horizontal (LVLH) frame attached to the reference (chief) spacecraft. Hill, Clohessy, and

<sup>1</sup> Department of Mechanics, Al-Farabi Kazakh National University, Almaty, 050040, Kazakhstan.

<sup>2</sup> Institute of Space Technique and Technology, Almaty 050061, Kazakhstan.

<sup>3</sup> Graduate School of Engineering, The University of Tokyo, Tokyo, 113-8656, Japan.

<sup>4</sup> Department of Intelligent Systems and Cybersecurity, Astana IT University, Astana, 010000, Kazakhstan.

\*Email: [nazgul.kaliyeva@gmail.com](mailto:nazgul.kaliyeva@gmail.com) (N. Kaliyeva); [y.shabdan@astanait.edu.kz](mailto:y.shabdan@astanait.edu.kz) (Y. Shabdan).

Wiltshire<sup>[15,16]</sup> developed a linear relative motion dynamic model by neglecting perturbation forces and assuming a uniform Earth gravitational field. Tschauner and Hempel<sup>[17]</sup> introduced a time-varying linearized dynamic model for the relative motion of deputy spacecraft concerning an elliptical reference orbit of the chief spacecraft. To enhance the accuracy of the relative motion dynamic model, third-body effects,<sup>[18]</sup> J2 perturbations<sup>[19-22]</sup>, and atmospheric drag<sup>[23-25]</sup> were taken into account. Clearly, models based on ordinary differential equations are convenient for controller design.

In this study, the Sedwick-Schweighart equations,<sup>[26]</sup> incorporating the J2 effect, were selected to describe the dynamics of the tetrahedron satellite formation in a geostationary orbit.

The challenge of maintaining the configuration of satellites within a formation in the presence of disturbances can be addressed through the synthesis of a control system. Numerous studies focus on controlling the motion of satellites in formations in low orbits. For instance, the authors of Ref. [27] proposed a solution to control a nanosatellite formation using  $H_\infty$  control theory. The outcome of the research yielded a nonlinear controller based on  $H_\infty$  control theory, ensuring asymptotic stability in the absence of orbital perturbations. In Ref. [28], a formation of two low-orbit satellites is explored, where the slave satellite is equipped with a passive orientation system providing uniaxial stabilization and a propulsion system with one or two engines oriented along a stabilized axis. The relative motion of the satellites is modeled using the linear Sedwick-Schweighart equations, considering the influence of J2 disturbances. It is demonstrated that, whether utilizing passive magnetic stabilization or uniaxial stabilization, there exists a control strategy ensuring periodic relative motion for all initial relative positions and velocities of the satellites. The study presented in Ref. [29] introduces an algorithm for controlling the flight of a satellite formation in low Earth orbit using aerodynamic force. A straightforward model of the aerodynamic force is proposed, accounting for the lift component. This enables the authors to calculate the satellite's orientation relative to the oncoming flow.

Several authors have addressed the challenge of maintaining the configuration of satellites within a formation in high geostationary orbit. In Ref. [25], a precise relative motion dynamic model of satellites in geostationary orbit is presented, utilizing Relative Orbital Elements (ROEs) while accounting for the J2 effect. The control system is developed using Linear Quadratic Regulator (LQR). Ref. [30] introduces the autonomous station/formation keeping of geostationary communications satellites, employing the IRNSS-based navigation and a high-fidelity perturbation model. In Ref. [31],

the authors explore the complete autonomous navigation and control of satellites in a cluster using the Hills-Clohessey-Wiltshire (HCW) equations.

In Ref. [32], the dynamics of formation flying, accounting for J2 perturbation and nonlinear dynamics, is examined utilizing a distributed game strategy. This study establishes a control strategy to achieve a desired formation configuration, minimize energy consumption, and mitigate the impact of disturbances on the formation system. The approach is based on the open-loop Nash/worst-case equilibrium strategy.

In Ref. [33], a comprehensive overview of spacecraft formation flight control is presented. The survey of formation modelling and control built on three methods. The first method is the multiple-input–multiple-output approach, where the formation is considered as a single entity with multiple inputs and multiple outputs. The second method is the leader–follower formation, where individual spacecraft controllers are interconnected hierarchically. Lastly, the virtual structure formation is explored, treating spacecraft as rigid bodies embedded in a common virtual rigid body.

A fuzzy control system was implemented for the formation. In Ref. [34], a fuzzy controller is employed in conjunction with a PD-controller for the motion control of spacecraft formations moving in elliptical orbits. Ref. [35] explores the application of low-thrust fuzzy control, utilizing the Clohessy-Wiltcher equations. The study compares this approach with optimal control using the "bang-bang" method and optimal control based on fuel and time consumption.

A robust controller for satellite formation flying subject to nonlinearity, parametric uncertainties, and external disturbances is presented in Ref. [36]. The proposed robust formation controller yields a position controller to form designed formation trajectories and patterns and an attitude controller to align satellite attitudes, for each satellite.

The above works are unique in the area of development of satellite formation motion control systems which give fairly good results. In this work, much attention is paid to the problem of development of the control system for maintaining the tetrahedral configuration of satellites formation in a geostationary orbit in the presence of disturbances caused by the influence of the inhomogeneity of the Earth's gravitational field. For this purpose it is planned to use more exact dynamic models such as Sedwick-Schweighart equations and more reliable control methods that will be described further.

Ref. [36] introduces a robust controller for satellite formation flying, accounting for nonlinearity, parametric uncertainties, and external disturbances. The proposed robust formation controller includes a position controller for shaping designed formation trajectories and patterns, as well as an

attitude controller for aligning satellite attitudes for each satellite.

These aforementioned studies stand out in the field of developing satellite formation motion control systems, delivering notably effective results. This present work places significant emphasis on addressing the challenge of synthesizing a control system to maintain the tetrahedral configuration of a satellite formation in geostationary orbit, particularly in the presence of disturbances caused by the influence of the inhomogeneity of the Earth's gravitational field. To achieve this, more precise dynamic models, such as the Sedwick-Schweighard equations, and reliable control methods will be employed.

## 2. Problem formulation and mathematical model of the motion of satellite in a tetrahedral formation

In this section, we consider the problem of synthesizing a control system for a small spacecraft formation in geostationary orbit. The formation comprises four spacecraft arranged in the shape of a tetrahedron or regular pyramid. In this configuration, the primary spacecraft is positioned above the three accompanying spacecraft located in the plane of the tetrahedron base, following an orbit referred to as the reference orbit (see Fig. 1). The accompanying spacecraft together form a regular triangle, with the height of the tetrahedron passing through the center of this triangle.

In the Fig. 1 are shown following coordinate systems for describing the motion of satellites formation:

OXYZ - inertial coordinate system (ICS), the center of which is located at the Earth's center of mass, the OZ axis is directed along the Earth's rotation axis, the OX is directed to the point of the Spring equinox of the J2000 epoch;

Cxyz – local vertical local horizontal coordinate system (LVLH), the center of which is in the reference satellite, the Ax axis is directed along the radius vector of the reference satellite from the center of the Earth, the Az axis is normal to the orbit plane in the direction of the orbital momentum, the Ay axis completes the system to the right.

As established in Ref. [37], in order to consider the Earth's gravitational field inhomogeneity, represented by the J2 zonal harmonic, it is necessary to express the gravitational potential in the following form<sup>[38]</sup>:

$$U_2 = -\frac{1}{2}\mu J_2 \frac{r_3^2}{R^3} (3\sin^2\varphi - 1) \quad (1)$$

where  $r_3$  is the radius of the Earth,  $R$  is the radius vector of the satellite in the ICS,  $\varphi$  is the latitude of the satellite in

the ICS,  $\mu$  is the Earth gravitational constant.

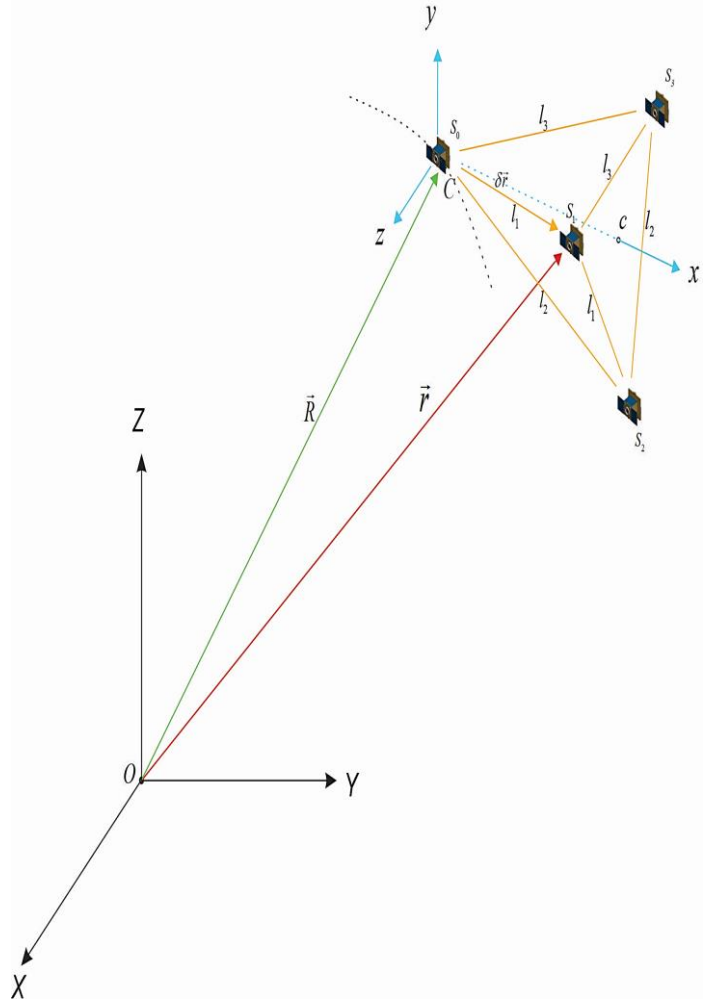


Fig. 1 Tetrahedral formation of satellites.

Further using (1) the equations of relative satellite motion in formation relative to the reference satellite in LVLH frame was derived in Ref. [18] in the form:

$$\ddot{x} - 2nc\dot{y} - (5c^2 - 2)n^2x = F_x, \quad \ddot{y} + 2nc\dot{x} = F_y, \quad (2)$$

$$\ddot{z} + q^2z = F_z + 2lq\cos(qt + \varphi),$$

where  $n = \sqrt{\frac{\mu}{R^3}}$ ,  $c = \sqrt{1 + s}$ ,  $s = \frac{3J_2r_3^2}{8R^3} (1 + 3\cos 2I)$ ,  $I$  is the orbit inclination of satellite in ICS,  $F_x, F_y, F_z$  are the forces caused by the  $J_2$ <sup>[18]</sup>:

$$F_x = -3n^2J_2 \frac{r_3^2}{R} \left( \frac{1}{2} - \frac{3I}{2} \frac{n^2(kt)}{2} - \frac{(1+3\cos 2I)}{8} \right),$$

$$F_y = -3n^2J_2 \frac{r_3^2}{R} \sin^2 I \sin(kt) \cos I \cos(kt), \quad (3)$$

$$F_z = 0,$$

$$k = nc + \frac{3\sqrt{\mu}J_2r_3^2}{R^{7/2}} \cos^2 I, \quad (4)$$

$$l = -R \frac{\sin \sin I_1 \sin \sin I_2 \sin \sin z_0}{R \sin \sin I \sin \sin [( \cos \cos I_1 \cos \cos I_2 + \sin \sin I_1 \sin \sin I_2 \cos \cos \Delta \Omega_0 )]} \left( \frac{3nJ_2r_3^2}{2R^2} \cos I_2 - \frac{3nJ_2r_3^2}{2R^2} \cos I_1 \right) \quad (5)$$

$$q \approx nc + \frac{3nJ_2r_s^2}{2R^2} \cos I_2, \tag{6}$$

where  $I_1, I_2$  is the inclination of orbits satellites in formation (it can be deputy and reference satellite),  $z_0 = z(0)$  is the initial value for coordinate  $z$  in relative position of satellites in formation,  $R$  is the radius-vector of reference satellite in ICS,  $I$  is the inclination of orbit of reference satellite.

To determine the extent of deviation of the current configuration from the tetrahedral one, we will rely on mathematical descriptions employed for calculating the volume of the tetrahedron and its quality factor<sup>[39]</sup>:

$$V_T = \frac{1}{6} \det|\vec{r}_1 - \vec{r}_0, \vec{r}_2 - \vec{r}_0, \vec{r}_3 - \vec{r}_0|, \tag{7}$$

where  $\vec{r}_0 = [x_0, y_0, z_0]$ ,  $\vec{r}_1 = [x_1, y_1, z_1]$ ,  $\vec{r}_2 = [x_2, y_2, z_2]$ ,  $\vec{r}_3 = [x_3, y_3, z_3]$  are the tetrahedron vertices given relative to the coordinate system with the origin at the geometric center of the tetrahedron.

$$Q = 12 \frac{(3V_T)^{2/3}}{L}, \tag{8}$$

where  $L$  is the sum of squares of the tetrahedron edge lengths  $L = (\vec{r}_1 - \vec{r}_2)^2 + (\vec{r}_1 - \vec{r}_3)^2 + (\vec{r}_2 - \vec{r}_3)^2 + \vec{r}_1^2 + \vec{r}_2^2 + \vec{r}_3^2$ . Quality factor equal to 1 in case of regular tetrahedron. When it less then 1 the configuration of regular tetrahedron is broken.

### 3. Control system for tetrahedron satellite formation

Let's formulate the equations for the controlled motion of a satellite in a formation in the form (2):

$$\begin{aligned} \ddot{x} - 2nc\dot{y} - (5c^2 - 2)n^2x &= F_x + u_x, \\ \ddot{y} + 2nc\dot{x} &= F_y + u_y, \end{aligned} \tag{9}$$

$\ddot{z} + q^2z = F_z + u_z + 2lq\cos(qt + \varphi)$ , where  $u_x, u_y, u_z$  are the control forces produced by actuators (thrusters).

In this work we assumed control force as linear function:

$$\begin{aligned} u_x &= -k_x(x - x_T) - k_{Vx}v_x, \\ u_y &= -k_y(y - y_T) - k_{Vy}v_y, \end{aligned} \tag{10}$$

$u_z = -k_z(z - z_T) - k_{Vz}v_z$ , where  $x_T, y_T, z_T$  are coordinates of required position of satellite in formation relative to the reference coordinate system,  $v_x, v_y, v_z$  are coordinates of relative velocity of satellites in formation. Additionally,  $k_x, k_{Vx}, k_y, k_{Vy}, k_z, k_{Vz}$  are constant coefficients.

To determine the unknown feedback coefficients  $k_x, k_{Vx}, k_y, k_{Vy}, k_z, k_{Vz}$  in expressions for control acceleration (10) we applied two methods. The first method utilized is the root locus method (RLM), which involves locating the roots of the characteristic equation of the system within specific regions of the complex plane.

As can be seen from (9) the third equation of the system does not involve the variables present in the first and second

equations. Therefore, it can be treated independently. We will seek a solution to the equation in the following form:

$$z = Ce^{\lambda t}. \tag{11}$$

From here we determine the corresponding values for  $\dot{z}, \ddot{z}$  and substitute these values into the third equation of system (9). After performing the necessary transformations, we arrive at an algebraic equation:

$$C(\lambda^2 + k_{Vy}\lambda + q^2 + k_y) = 0. \tag{12}$$

Obviously, equation (12) is a second-degree polynomial in the following form:

$$a_0\lambda^2 + a_1\lambda + a_2 = 0 \tag{13}$$

Let's consider the first and second equations of the system (9). We will seek solutions for them in the following form:

$$x = Ae^{\lambda t}, y = Be^{\lambda t}. \tag{14}$$

determine the corresponding time derivatives and substitute them into the equations of the system (9). After performing the necessary transformations, we obtain the corresponding system of algebraic equations:

$$\begin{aligned} A(\lambda^2 + k_{Vx}\lambda + k_x - (5n^2c^2 - 2n^2)) - 2nc\lambda B &= 0, \\ B(\lambda^2 + k_{Vy}\lambda + k_y) + 2nc\lambda A &= 0. \end{aligned} \tag{15}$$

Since the system of equations (15) must possess a non-zero solution for both A and B, the determinant of this system is required to be equal to zero:

$$\begin{aligned} |\lambda^2 + k_{Vx}\lambda + k_x - (5n^2c^2 - 2n^2) - 2nc\lambda \quad 2nc\lambda \lambda^2 + \\ k_{Vy}\lambda + k_y| = 0 \end{aligned} \tag{16}$$

or

$$\begin{aligned} \lambda^4 + \lambda^3(k_{Vx} + k_{Vy}) + \lambda^2 \left( \frac{k_x + k_y + k_{Vx}k_{Vy} -}{(5n^2c^2 - 2n^2) - 4n^2c^2} \right) + \\ + \lambda(k_xk_{Vy} + k_{Vx}k_y - k_{Vy}(5n^2c^2 - 2n^2)) + k_xk_y - \\ (5n^2c^2 - 2n^2)k_y = 0 \end{aligned} \tag{17}$$

$$a_0\lambda^4 + a_1\lambda^3 + a_2\lambda^2 + a_3\lambda + a_4 = 0. \tag{18}$$

We define the required roots of the second-order characteristic equation as the roots of the Butterworth polynomial in the form:

$$\lambda^2 + 1.414\Omega_r\lambda + \Omega_r^2 = 0, \tag{19}$$

where  $\Omega_r = \frac{t_H}{t_p}$ ,  $t_H$  is the normalized time of the transient process,  $t_p$  - is the real time of the transient process.

And the roots of the fourth-order characteristic equation are defined as the roots of the Butterworth polynomial in the following form:

$$\lambda^4 + 2.613\Omega_r\lambda^3 + 3.4141\Omega_r^2\lambda^2 + 2.613\Omega_r^3\lambda + \Omega_r^4 = 0 \tag{20}$$

By further equating terms at the similar power of  $\lambda$  in formulas (12) and (19), we derive expressions for determining the unknown feedback coefficients:

$$k_{Vy} = 1.414\Omega_r, k_y = \Omega_r^2 - q^2 \quad (21)$$

By equating terms at the similar power of  $\lambda$  in formulas (17) and (20), we obtain a system of algebraic equations for determining the unknown feedback coefficients:

$$k_{Vx} + k_{Vy} = 2.613\Omega_r,$$

$$k_x + k_y + k_{Vx}k_{Vy} - (5n^2c^2 - 2n^2) - 4n^2c^2 = 3.4141\Omega_r^2$$

$$k_xk_{Vy} + k_{Vx}k_y - k_{Vy}(5n^2c^2 - 2n^2) = 2.613\Omega_r^3, \quad (22)$$

$$k_xk_y - (5n^2c^2 - 2n^2)k_y = \Omega_r^4.$$

Using the parameters of the reference unperturbed orbit of the main satellite in the form: the radius of the circular orbit is 42000 km, the inclination  $I = 0^0$ , we derive the following results:

$$n = 0.00007293976184, c = 1.000017129,$$

$$q = 0.00007294351003. \quad (23)$$

With the parameters (23), by solving equations (21), (22), the feedback coefficients were determined by solving equations (21) and (22) using the root method (RLM):

$$\begin{aligned} k_x &= 1.4400, k_{Vx} = 1.7125, \\ k_y &= 0.7075, k_{Vy} = 1.4209, \\ k_z &= 0.7961, k_{Vz} = 1.4986. \end{aligned} \quad (24)$$

The second method to determine the unknown feedback coefficients  $k_x, k_{Vx}, k_y, k_{Vy}, k_z, k_{Vz}$  in equation (10), aimed at maintaining the motion of the satellite at a certain distance from the center of the formation, involves the use of a Linear Quadratic Regulator (LQR). This regulator is obtained by minimizing a quality criterion in the following form<sup>[40]</sup>:

$$J = \frac{1}{2} \int (\overline{\Delta r}^T Q \overline{\Delta r} + \overline{u}^T R \overline{u}) dt \quad (25)$$

where  $\overline{\Delta r} = [x - x_T, y - y_T, z - z_T, v_x, v_y, v_z]$ ,  $Q, R$  are positive matrices with constant components,  $x_T, y_T, z_T$  are the required position of the satellite in a formation.

The linear quadratic performance criterion is applicable to linear systems of the form:

$$\dot{\vec{X}} = A\vec{X} + B\vec{u}, \quad (26)$$

where  $\vec{X}$  is the state vector,  $A$  is the system matrix,  $B$  is the control matrix.

We bring equations (9) to the form (26):

$$\begin{aligned} \dot{x} &= v_x, \dot{y} = v_y, \dot{z} = v_z, \\ \dot{v}_x &= 2ncv_y + (5c^2 - 2)n^2x + u_x, \\ \dot{v}_y &= -2ncv_x + u_y, \dot{v}_z = -q^2z + u_z. \end{aligned} \quad (27)$$

For equations of the form (27), the matrices  $A$  and  $B$  have the form:

$$A = [0 \ 0 \ 0 \ (5c^2 -$$

$$\begin{aligned} &2)n^2 \ 0 \ 0 \ 0 \ 0 \ 0 \ 0 \ 0 \ 0 \ 0 \ 0 \ -q^2 \ 1 \ 0 \ 0 \ 0 \ - \\ &2nc \ 0 \ 0 \ 1 \ 0 \ 2nc \ 0 \ 0 \ 0 \ 0 \ 1 \ 0 \ 0 \ 0], \end{aligned} \quad (28)$$

$$B = [0 \ 0 \ 0 \ 1 \ 0 \ 0 \ 0 \ 0 \ 0 \ 1 \ 0 \ 0 \ 0 \ 0 \ 0 \ 1]. \quad (29)$$

The control acceleration  $\vec{u} = [u_x, u_y, u_z]$ , obtained by minimizing the performance criterion (25), takes the following form:

$$\vec{u} = -R^{-1}B^T P \overline{\Delta r} = K \overline{\Delta r}, \quad (30)$$

where the matrix  $R$  has the form:

$$R = 0.0001 \cdot \text{diag}[1, 1, 1]. \quad (31)$$

The matrix  $P$  can be determined from the following equation:

$$A^T P + PA - PBR^{-1}B^T P + Q = 0. \quad (32)$$

$$Q = 0.0001 \cdot \text{diag}[1, 1, 1, 1, 1, 1]. \quad (33)$$

As a result of solving equations (32), the matrix of feedback coefficients is determined using the LQR method (Fig. 2):

$$K = [k_x \ 0 \ 0 \ 0 \ k_y \ 0 \ 0 \ 0 \ k_z \ k_{Vx} \ 0 \ 0 \ 0 \ k_{Vy} \ 0 \ 0 \ 0 \ k_{Vz}], \quad (34)$$

where

$$\begin{aligned} k_x &= 1.0000, k_{Vx} = 1.7321, \\ k_y &= 0.9999, k_{Vy} = 1.7321, \\ k_z &= 0.9999, k_{Vz} = 1.7320. \end{aligned} \quad (35)$$

#### 4. The results and discussion of the numerical simulation for tetrahedron satellite formation

To validate the obtained control system, a numerical solution of equations (9) was performed using initial conditions that define the positions of the four satellites relative to their geometric center (Table 1).

The results of the numerical studies are illustrated in the figures below. As the required position of the satellites in a formation  $x_T, y_T, z_T$ , we set the initial conditions given above. Figures 3-8 show the results of numerical calculations of the mutual distances between the satellites using two control methods, RLM and LQR, within a single time interval.

The accuracy in plotting results from the small distances between the satellites, which are necessary for implementing the Fizeau interferometer in a geostationary orbit.

In many cases, the amplitude of satellite oscillations is greater with the RLM method, except for  $l_{01}$  and  $l_{23}$ . Additionally, it is important to note that the decay time of oscillations with LQR is several units shorter than when using the RLM control algorithm. This aspect is crucial for the successful completion of the mission.

In Fig. 3, it can be observed that the RLM control algorithm, quasi-periodic oscillations of the satellite S1 are present relative to its initial position. In the case of the LQR control method there is a pronounced aperiodic motion, which is also reflected in the dynamics of the formation volume and the quality factor -  $Q$  (see Figs. 9 and 10). The observed difference in the use of different control methods occurs at smaller scales,

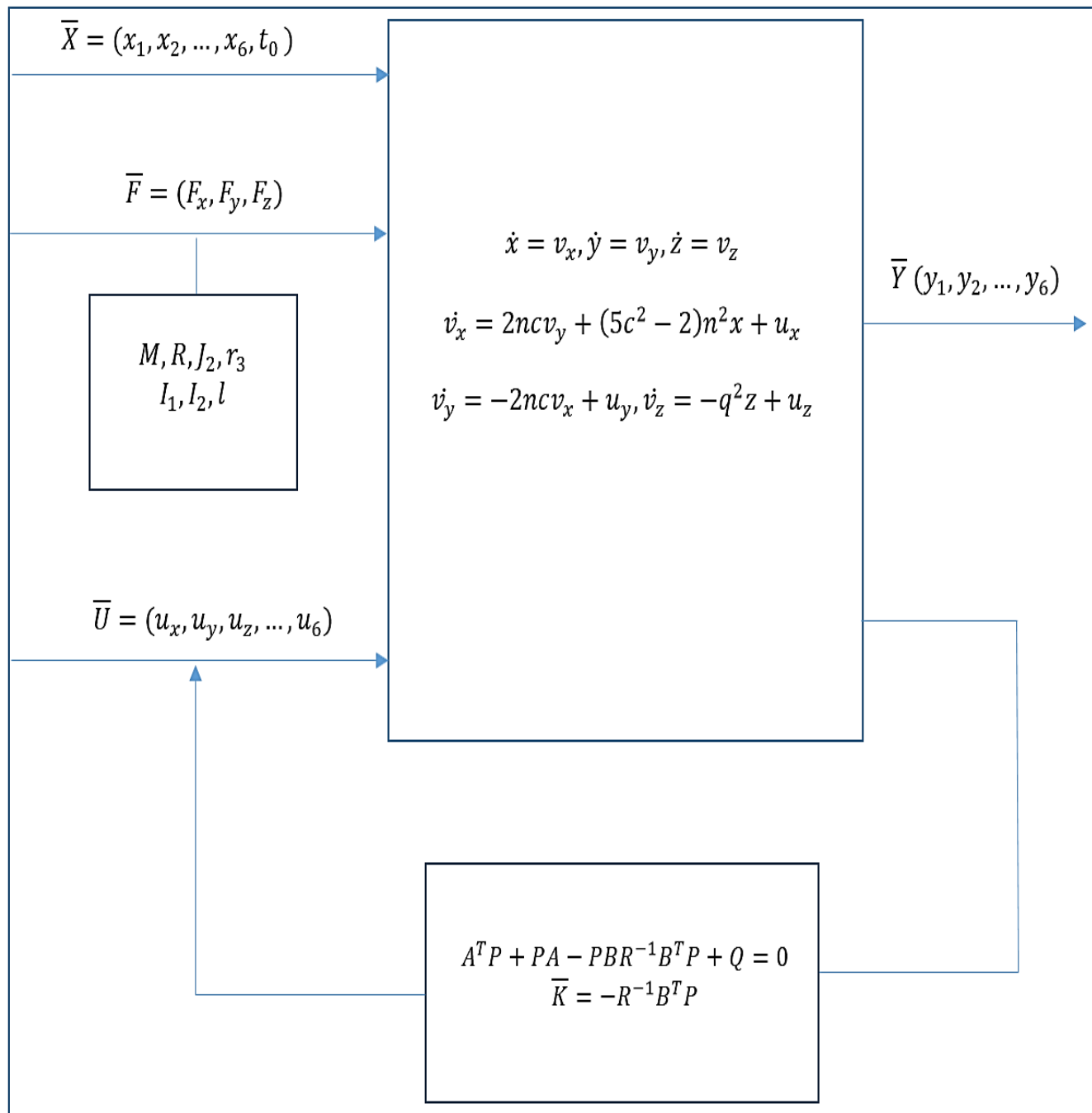
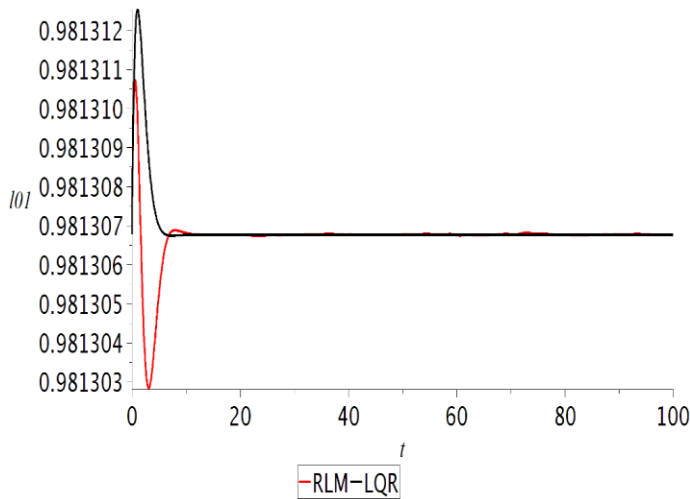


Fig. 2 LQR control algorithm flowchart.

Table 1. Initial conditions specifying the positions of the four satellites relative to their geometric center.

Initial position (m) and velocity (m/s), X axis	Initial position (m) and velocity ( $\mu\text{m/s}$ ), Y axis	Initial position (m) and velocity (m/s), Z axis
$x_0(t_0) = -0.5443$	$y_0(t_0) = 0$	$z_0(t_0) = 0$
$x_1(t_0) = 0.2722$	$y_1(t_0) = 0$	$z_1(t_0) = 0.5443$
$x_2(t_0) = 0.2722$	$y_2(t_0) = -0.4082$	$z_2(t_0) = -0.2722$
$x_3(t_0) = 0.2722$	$y_3(t_0) = 0.4082$	$z_3(t_0) = -0.2722$
$v_{0x}(t_0) = -3074.1405$	$v_{0y}(t_0) = 39.6932$	$v_{0z}(t_0) = 0$
$v_{1x}(t_0) = -3074.1405$	$v_{1y}(t_0) = -19.8466$	$v_{1z}(t_0) = 0$
$v_{2x}(t_0) = -3074.1405$	$v_{2y}(t_0) = -19.8466$	$v_{2z}(t_0) = 0$
$v_{3x}(t_0) = -3074.1405$	$v_{3y}(t_0) = -19.8466$	$v_{3z}(t_0) = 0$

due to disturbances arising from the inhomogeneity of the Earth's gravitational field.



**Fig. 3** The distance between satellites S0 and S1.

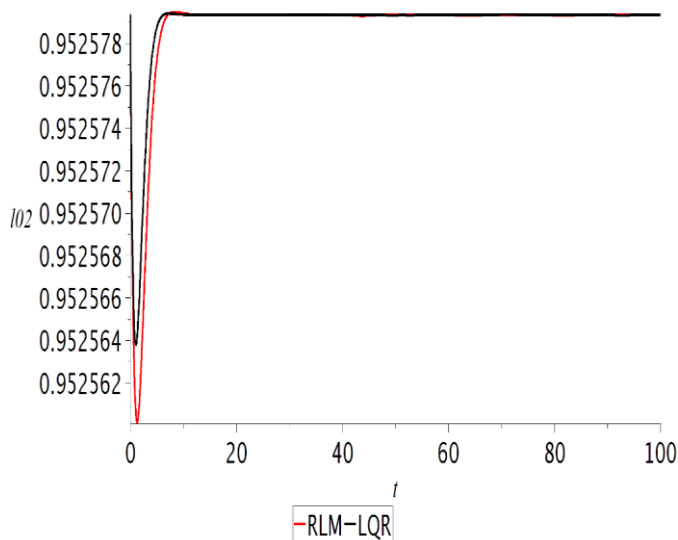


**Fig. 4** The distance between satellites S0 and S2.

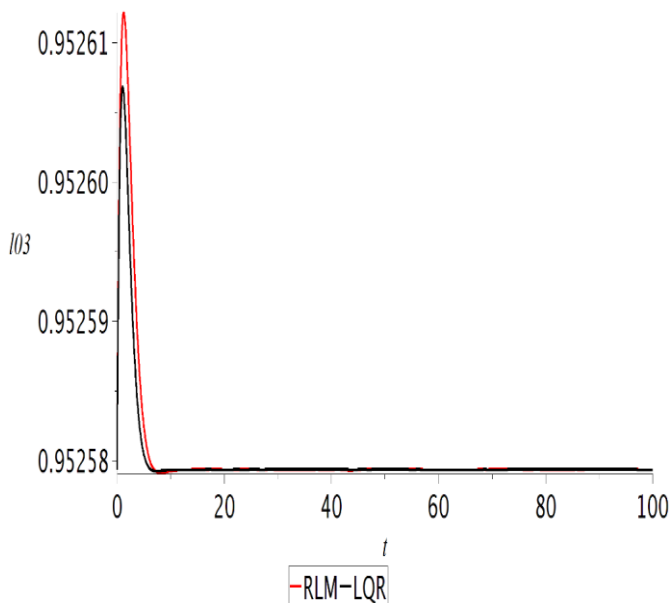


**Fig. 5** The distance between the satellites S0 and S3.

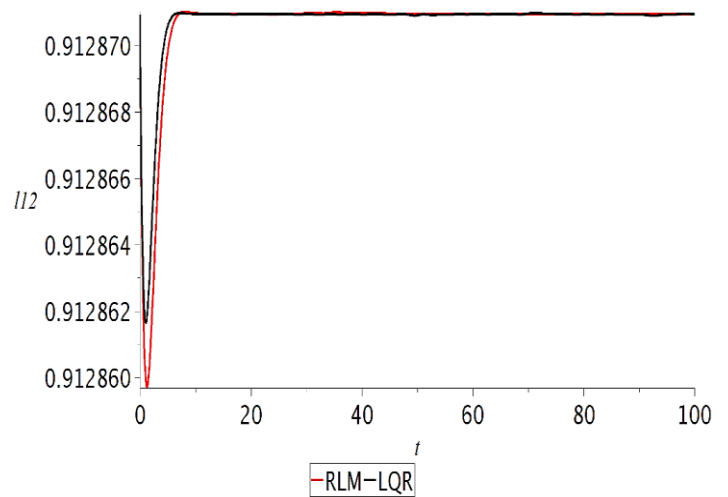


**Fig. 6** The distance between satellites S1 and S2.

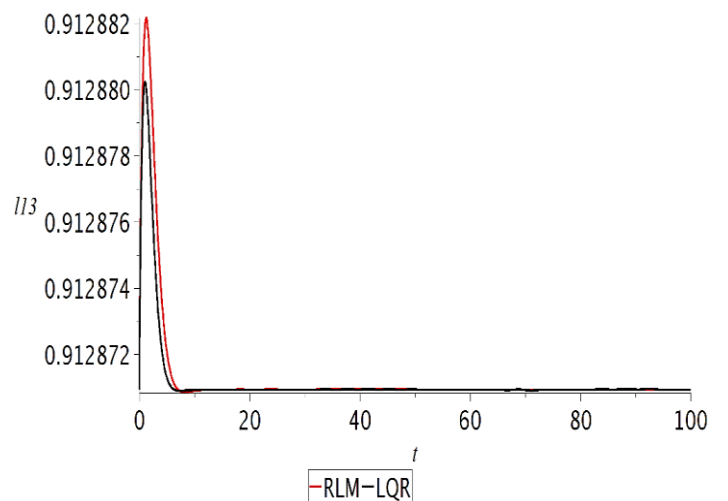


**Fig. 7** The distance between satellites S1 and S3.

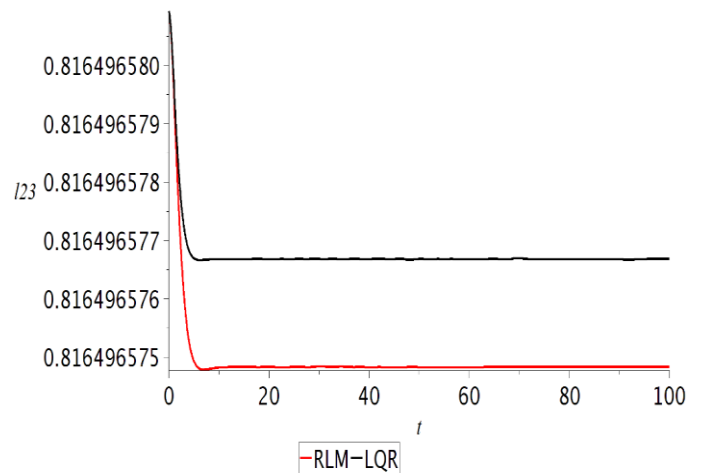


**Fig. 8** The distance between the satellites S3 and S2.

As seen in the figures, the stabilization of the triangular configuration occurs within the period of 15-20 seconds under the influence of external perturbing gravitational force and control force. The obtained results confirm that, when control actions are applied, the initial configuration is maintained throughout the entire time interval of 100 seconds and beyond.

Simultaneously, it is evident that the control action based on LQR allows achieving the required position of the satellites in a configuration with a smaller overshoot compared to RLM (0.002%).

Figures 9-10 show the results of the numerical calculation of the volume and quality factor of the formation during the first 15 seconds. The obtained results demonstrate that impact of external forces caused by the inhomogeneity of the Earth are leveled out during the initial stage of motion. Throughout the subsequent period, the formation volume and quality factor consistently maintain values within the specified requirements.

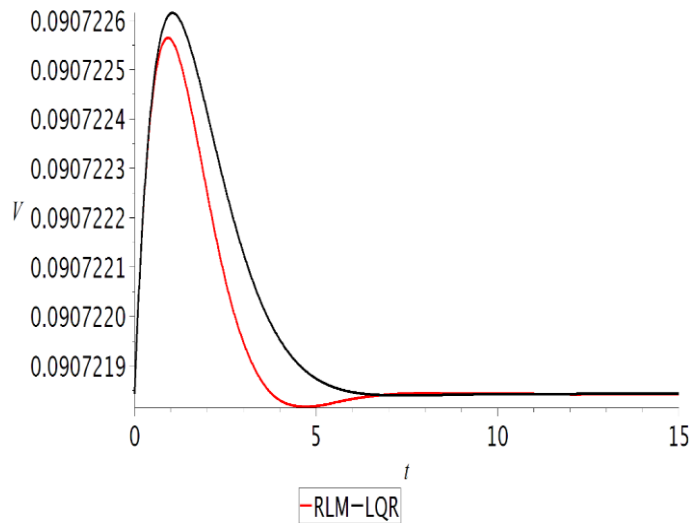


Fig. 9 The volume of formation.

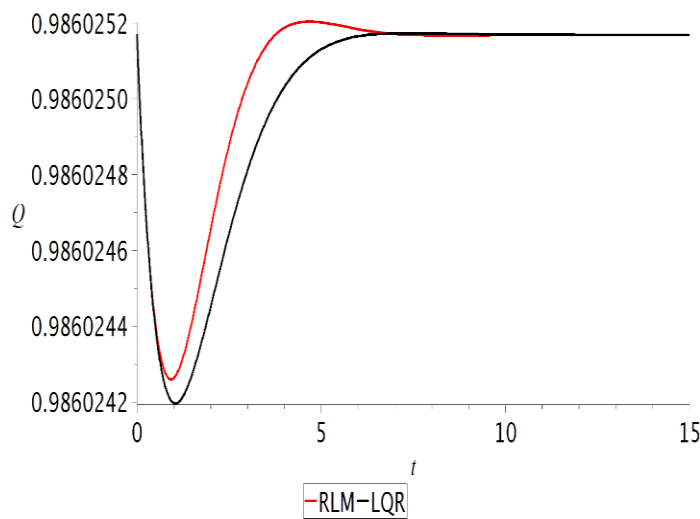


Fig. 10 The quality factor of formation.

Figures 11-14 illustrate the results of the numerical calculation of the control forces necessary to maintain the formation.

As evident from Figs. 11-14, the maximum control force required to maintain the satellite formation configuration is 0.007 N or 7 mN. Let's explore the potential actuator capable of generating such force to preserve the formation. In this

study, it is assumed that three accompanying spacecraft located in the plane of the tetrahedron base (S1, S2, S3 - see Fig. 1) are small, each weighing up to 50 kg. The central satellite, S0 (Fig. 1), has a weight of 65 kg. Drawing on contemporary literature regarding actuators employed in small satellite missions, electric propulsion systems are deemed more suitable than classical chemical systems. This preference is due to their lower payload mass requirement for fuel and their ability to extend the mission's lifetime. Assuming that each satellite in the configuration can produce a maximum power of 800 W through solar arrays, a fraction of this power, up to 200 W, is designated for the electric propulsion systems. Currently, various types of electric propulsion systems are available for use on small satellites, including electrostatic, electrothermal, and electromagnetic systems. In the case of electrostatic thrusters, electrical power is initially utilized to ionize the propellant, leading to plasma production. The ions are then accelerated through electrodes that apply an electric field for plasma acceleration.<sup>[41]</sup> Electrospray thrusters, for instance, operate in either droplet or ion emission mode, and field emission electric propulsion thrusters emit individual ions, requiring a neutralizer as they operate with a liquid metal. Gridded ion thrusters generate ions by bombarding a propellant with a high-energy electron beam created through direct current discharge, radio frequency discharge, or microwave discharge.<sup>[41,42]</sup> Hall thrusters accelerate the propellant to high velocity as it passes through an electric field in a channel generated perpendicular to the magnetic field.<sup>[41,42]</sup> In electrothermal systems, electrical power is used to heat the propellant in a chamber. The heated propellant is then expanded through a converging/diverging nozzle for acceleration.<sup>[41]</sup> Electromagnetic systems ionize and accelerate the propellant under the combined influence of magnetic and electric fields. Consequently, these systems often require higher power levels.<sup>[41]</sup>

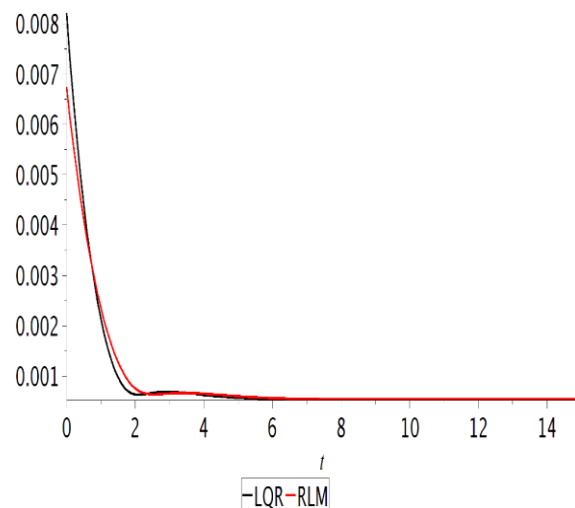


Fig. 11 The value of force acting on satellite S0.



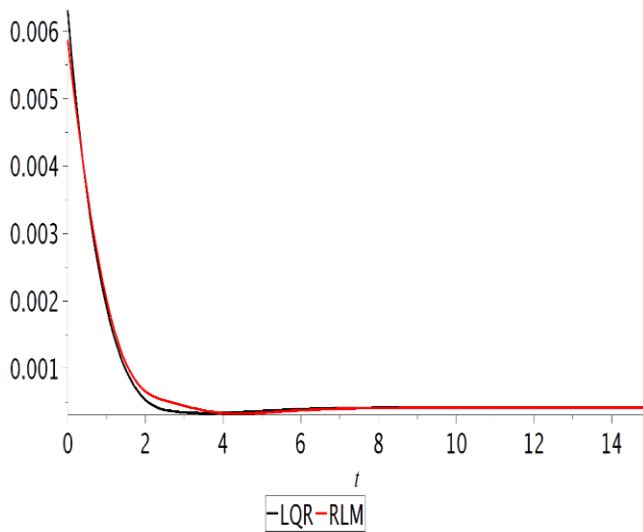


Fig. 12 The value of force acting on satellite S1.

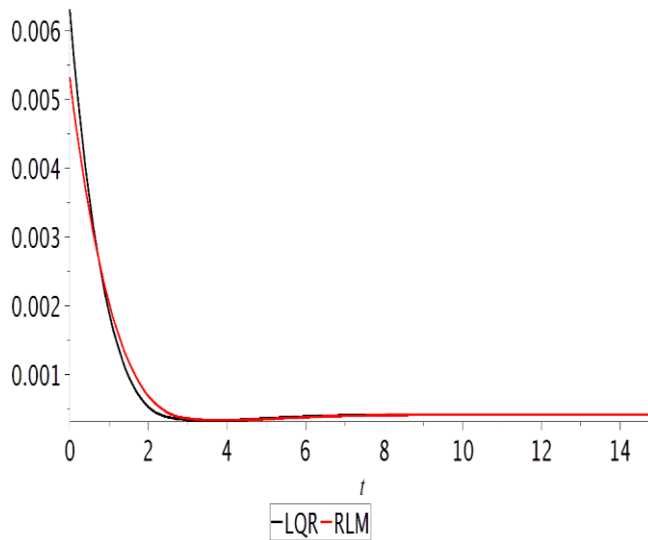


Fig. 13 The value of force acting on satellite S2.

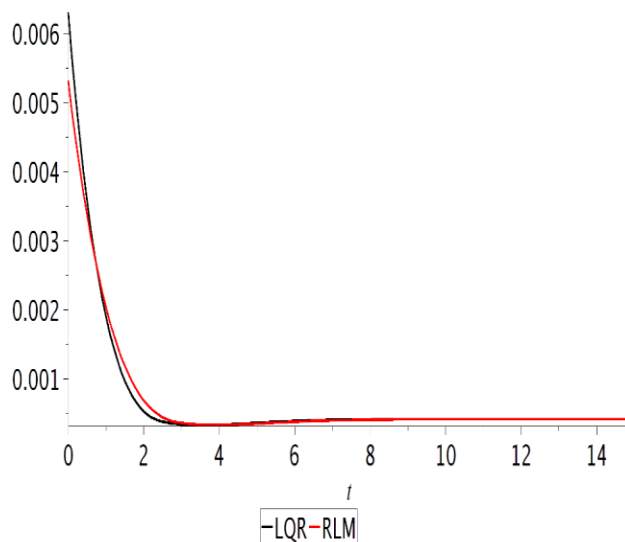


Fig. 14 The value of force acting on satellite S3.

Thrust of electrostatic, electrothermal and electromagnetic propulsion systems can be generally estimated by selecting an

arbitrary specific impulse  $I_{sp}$ , the thrust efficiency  $\eta_t$  and the power input  $P_t$ <sup>[41]</sup>:

$$\tau = \frac{2\eta_t P_t}{I_{sp} g_0}, \tag{36}$$

where  $g_0$  is the gravity due to Earth.

Considering that we focused on thrusters with a power consumption of up to 200 W, let's explore the types of thrusters that could be suitable for our problem. Regarding commercially available electric propulsion systems, such as electrostatic gridded ion thrusters and Hall thrusters with input power up to 200 W, the specific impulse varies from 1300 s to 3000 s.<sup>[41]</sup> This implies that the maximum generated thrust is about 0.015 N or 15 mN, and the minimum generated thrust is about 0.0066 N or 6.6 mN. Comparing these thrust values with the maximum control force requirement of 7 mN to maintain the satellite configuration, we can conclude that the mathematical framework developed in this paper can be implemented in the control system of a satellite formation in geostationary orbit to effectively control the motion of satellites within the formation and their relative positions.

### 5. Conclusions

This paper addresses the motion and maintenance of a tetrahedral formation of satellites, representing a Fizeau interferometer configuration in geostationary orbit. The formation consists of three small satellites, each weighing up to 50 kg, positioned in the plane of the tetrahedron base. The top satellite of the tetrahedron weighs 65 kg. A notable aspect is that 25% of the generated power of each satellite is allocated for electric propulsion systems.

Two algorithms, based on the root locus method and linear quadratic regulator, were investigated for maintaining the tetrahedral configuration. An assessment of the applicability of these algorithms in controlling the motion of satellites within the formation was conducted. The numerical study revealed that the developed control methods for satellite motion in a formation could effectively extend to regulating the relative positions of satellites within a Fizeau interferometer configuration in geostationary orbits, particularly when utilizing modern electric propulsion systems.

### Acknowledgements

This work was supported by grant funding within the framework of the project AP09260469 Development of a control system for configuration keeping of the spacecraft formation with taking into account the uncertainties.

### Conflict of Interest

There is no conflict of interest.

## Supporting Information

Not applicable.

## References

- [1] G. Tyc, K. Ruthman, P. Stephens, A. Wicks, T. Butlin, M. Krischke, M. Oxford, RapidEye - an Earth observation smallsat constellation for daily agricultural monitoring, Proceedings of the 17th AIAA/USU Conference on Small Satellites, 2003.
- [2] W. Yi, Y. Wang, Y. Zeng, Y. Wang, J. Xu, Comprehensive evaluation of the GF-4 satellite image quality from 2015 to 2020, *ISPRS International Journal of Geo-Information*, 2021, **10**, 406, doi: 10.3390/ijgi10060406.
- [3] L. Mugnier, F. Cassaing, G. Rousset, F. Baron, V. Michau, I. Mocœur, B. Sorrente, M-T. Velluet, continuous high-resolution earth observation with multiple aperture optical telescopes, Proceedings of the OPTRO 2005 International Symposium, 2005.
- [4] F. Hénault, Imaging and nulling properties of sparse-aperture Fizeau interferometers, *Optical and Infrared Interferometry IV*. SPIE, 2014, **9146**, 366-379, doi: 10.1117/12.2055069.
- [5] G. Rousset, L. M. Mugnier, F. Cassaing, B. Sorrente, Imaging with multi-aperture optical telescopes and an application, *Comptes Rendus De L'Académie Des Sciences - Series IV - Physics*, 2001, **2**, 17-25, doi: 10.1016/S1296-2147(01)01158-1.
- [6] M. Mesrine, E. Thomas, S. Garin, P. Blanc, C. Alis, F. Cassaing, D. Laubier, High resolution earth observation from geostationary orbit by optical aperture synthesys, Proceedings SPIE 10567, International Conference on Space Optics — ICSSO 2006, 2017, **10567**, 71-77, doi: 10.1117/12.2308095.
- [7] D. Dolkens, J. M. Kuiper, A deployable telescope for sub-meter resolutions from microsatellite platforms, Proceedings SPIE 10563, International Conference on Space Optics — ICSSO 2014, 2017, **10563**, 992-1000, doi: 10.1117/12.2304245.
- [8] S. Cui, B. Xu, S. Luo, H. Xu, Z. Cai, Z. Luo, J. Pu, S. Chávez-Cerda, Determining topological charge based on an improved Fizeau interferometer, *Optics Express*, 2019, **27**, 12774-12779, doi: 10.1364/OE.27.012774.
- [9] L. M. Mugnier, F. Cassaing, G. Rousset, B. Sorrente, Earth observation from a high orbit: pushing the limits with synthetic aperture optics, Proceedings of the Space-based observation techniques, 2000.
- [10] A. D. Ogundele, Modeling and analysis of nonlinear spacecraft relative motion via harmonic balance and Lyapunov function, *Aerospace Science and Technology*, 2020, **99**, 105761, doi: 10.1016/j.ast.2020.105761.
- [11] G. Inalhan, J. How, Relative dynamics and control of spacecraft formations in eccentric orbits AIAA Guidance, Navigation, and Control Conference and Exhibit. 14 August 2000 - 17 August 2000, Dever, CO. Reston, Virginia: AIAA, 2000: 4443, doi: 10.2514/6.2000-4443.
- [12] R. G. Melton, Time-explicit representation of relative motion between elliptical orbits, *Journal of Guidance, Control, and Dynamics*, 2000, **23**, 604-610, doi: 10.2514/2.4605.
- [13] P. Gurfil, N. J. Kasdin, Nonlinear modelling of spacecraft relative motion in the configuration space, *Journal of Guidance, Control, and Dynamics*, 2004, **27**, 154-157, doi: 10.2514/1.9343.
- [14] A. D. Ogundele, Nonlinear dynamics and control of spacecraft relative motion, Ph.D. Thesis, Aerospace engineering department, Auburn University, 2017.
- [15] G. W. Hill, Researches in the lunar theory, *American Journal of Mathematics*, 1878, **1**, 5-26, doi: 10.2307/2369430.
- [16] W. H. Clohessy, R. S. Wiltshire, Terminal guidance system for satellite rendezvous, *Journal of the Aerospace Sciences*, 1960, **27**, 653-658, doi: 10.2514/8.8704.
- [17] J. Tschauner, P. Hempel, Rendezvous zu einem in elliptischer bahn umlaufenden ziel [Rendezvous with a Target in an Elliptical Orbit], *Acta Astronautica*, 1965, **2**, 104-109.
- [18] S. A. Schweighart, R. J. Sedwick, High-fidelity linearized J model for satellite formation flight, *Journal of Guidance, Control, and Dynamics*, 2002, **25**, 1073-1080, doi: 10.2514/2.4986.
- [19] K. T. Alfriend, H. Schaub, Dynamic and control of spacecraft formations: challenges and some solutions, *The Journal of the Astronautical Sciences*, 2000, **48**, 249-267, doi: 10.1007/BF03546279.
- [20] J. Marsden, W. Koon, R. Murray, J. Masdemont, J2 dynamics and formation flight AIAA Guidance, Navigation, and Control Conference and Exhibit. 06 August 2001 - 09 August 2001, Montreal, Canada. Reston, Virginia: AIAA, 2001: 4090, doi: 10.2514/6.2001-4090.
- [21] J.S. Ginn, Spacecraft formation flight analysis of the perturbed J2-modified Hill-Clohessy-Wiltshire equations, Master Thesis, The University of TEXAS at Arlington, 2006.
- [22] H. Schaub, Incorporating secular drifts into the orbit element difference description of relative orbits, *Advances in The Astronautical Sciences*, 2003, **114**, 239-257.
- [23] R. J. Sedwick, D. W. Miller, E. M. C. Kong, Mitigation of differential perturbations in formation flying satellite clusters, *The Journal of the Astronautical Sciences*, 1999, **47**, 309-331, doi: 10.1007/BF03546206.
- [24] T. Carter, M. Humi, Clohessy-wiltshire equations modified to include quadratic drag, *Journal of Guidance, Control, and Dynamics*, 2002, **25**, 1058-1063, doi: 10.2514/2.5010.
- [25] L. Rizzieri, Relative motion control of cluster formation in a geostationary orbit with the J22 perturbation, Master Thesis, Politecnico di Milano, 2022.
- [26] J. Li, X. Meng, Y. Gao, X. Li, Study on relative orbital configuration in satellite formation flying, *Acta Mechanica Sinica*, 2005, **21**, 87-94, doi: 10.1007/s10409-004-0009-3.
- [27] B. Naasz, C.D. Karlgaard, C. Hall, Application of several control techniques for the ionospheric observation nanosatellite formation, *Advances in the Astronautical Sciences*, 2002, **112**, 1063-1079.
- [28] A. Guerman, M. Ovchinnikov, G. Smirnov, S. Trofimov, Closed relative trajectories for formation flying with single-input control, *Mathematical Problems in Engineering*, 2012, **2012**, 967248, doi: 10.1155/2012/967248.
- [29] D. Ivanov, M. Kushniruk, M. Ovchinnikov, Study of satellite formation flying control using differential lift and drag, *Acta Astronautica*, 2018, **152**, 88-100, doi: 10.1016/j.actaastro.2018.07.047.

- [30] V. Kumar, H. B. Hablani, Autonomous formation keeping of geostationary satellites with regional navigation satellites and dynamics, *Journal of Guidance, Control, and Dynamics*, 2017, **40**, 563-583, doi: 10.2514/1.G001652.
- [31] V. Kumar, H. Hablani, Relative motion control of geostationary satellites in formation, *Advances in the Astronautical Sciences*, 2012, **145**, 1343-1351.
- [32] J. Li, S. Chen, C. Li, F. Wang, Distributed game strategy for formation flying of multiple spacecraft with disturbance rejection, *IEEE Transactions on Aerospace and Electronic Systems*, 2021, **57**, 119-128, doi: 10.1109/TAES.2020.3010593.
- [33] B. Andrievsky, A. M. Popov, I. Kostin, J. Fadeeva, Modeling and control of satellite formations: a survey, *Automation*, 2022, **3**, 511-544, doi: 10.3390/automation3030026.
- [34] P. Wang, D. Yang, PD-fuzzy formation control for spacecraft formation flying in elliptical orbits, *Aerospace Science and Technology*, 2003, **7**, 561-566, doi: 10.1016/S1270-9638(03)00055-5.
- [35] Q. Meng, P. Wang, D. Yang, Low-thrust fuzzy formation keeping for multiple spacecraft flying, *Acta Astronautica*, 2004, **55**, 895-901, doi: 10.1016/j.actaastro.2004.04.007.
- [36] H. Liu, Y. Tian, F. L. Lewis, Y. Wan, K. P. Valavanis, Robust formation flying control for a team of satellites subject to nonlinearities and uncertainties, *Aerospace Science and Technology*, 2019, **95**, 105455, doi: 10.1016/j.ast.2019.105455.
- [37] C. Xu, R. Tsoi, N. Sneeuw, Analysis of J2-perturbed relative orbits for satellite formation flying, *International Association of Geodesy Symposia*, Berlin/Heidelberg: Springer-Verlag, 2005, 30-35, doi: 10.1007/3-540-26932-0\_6.
- [38] A. E. Roy, *Orbital Motion*, CRC Press, 2020.
- [39] A. Liu, B. Joe, On the shape of tetrahedra from bisection, *Mathematics of Computation*, 1994, **63**, 141-154, doi: 10.2307/2153566.
- [40] Z. Rakisheva, A. Sukhenko, N. Kaliyeva, Optimization issues in the problem of small satellite attitude determination and control. Fasano G, Pintér J, Modeling and Optimization in Space Engineering. Cham: Springer, 2019, 373-393, doi: 10.1007/978-3-030-10501-3\_14
- [41] D. O'Reilly, G. Herdrich, D. F. Kavanagh, Electric propulsion methods for small satellites: a review, *Aerospace*, 2021, **8**, 22, doi: 10.3390/aerospace8010022.
- [42] V. Zakirov, M. Sweeting, P. Erichsen, T. Lawrence, Specifics of small satellite propulsion: part 1, In proceedings of 15th AIAA/USU conference on small satellites, USA, Utah, 2001.

**Publisher's Note:** Engineered Science Publisher remains neutral with regard to jurisdictional claims in published maps and institutional affiliations.